JOURNAL OF MATERIALS SCIENCE **40** (2005) 43–46

Preparation and thermal characteristics of silane-grafted polyethylene/montmorillonite nanocomposites

HONGDIAN LU[‡], YUAN HU[‡,*], LING YANG[‡], ZHENGZHOU WANG[‡], ZUYAO CHEN[§], WEICHENG FAN[‡]
[‡]*State Key Laboratory of Fire Science and* [§]*Department of Chemistry, University of Science and Technology of China, Hefei, 230026, Anhui, People's Pepublic of China*
E-mail: yuanhu@ustc.edu.cn

Intercalated methacryloylpropyltrimethoxysilane (VMMS)-grafted polyethylene (PE-g-VMMS) /organo-montmorillonite (OMT) nanocomposite was prepared by melt intercalation. Its morphology and thermal characteristics were carried out by X-ray diffraction (XRD), transmission electron microscopy (TEM), thermogravimetric analyses (TGA) and dynamic Fourier transfer infrared (FTIR) spectroscopy. The intercalated tactoids of silicate layers within PE-g-VMMS have been verified by XRD and TEM image. TGA profiles of the nanocomposite show that the presence of the silicates exerts a significant stabilization effect on thermal-oxidative degradation process from 250 to 375°C, but less effect above 375°C. Dynamic FTIR spectra reveal that this nanocomposite has a slower thermal-oxidative degradation rate of main chains than that of pure PE-g-VMMS, but a faster rate of the pendant VMMS grafts.

1. Introduction

Polymer/clay nanocomposites where nanoscale silicate layers are molecularly dispersed within the polymeric matrix exhibit dramatic concurrent enhancements of mechanical, thermal stability, flame retardancy, and barrier properties even when employing small loading levels of clay (<10 wt%) when compared to pure polymer [1]. Therefore, since such nanocomposites were reported by the Toyota group, more research has been done in this field [2].

Polyolefins including polyethylene (PE) and polypropylene (PP) have been tested for the preparation of nanocomposites [3–12]. However, it is difficult to fabricate the nanostructure of polyolefins with simply amino acids or alkylammonium salts modified silicate layers due to the nonpolarity of polyolefin chains [7, 8]. To facilitate interaction of polyolefins with the modified layers, introduction of polymer modified with maleic anhydride or hydroxyl groups as a compatibilizer to mediate the polarity between the polymer and the alkylammonium exchanged montmorillonite is often employed [9, 10].

It is known that silane grafting is an important way to functionalize polyolefins, particular for the preparation of silane-grafted water-crosslinked polyethylene [13–15]. Moreover, as far as we are aware, many researches have been focused on the modification of clay with alkoxysilanes and the formation of covalently bonds by grafting alkoxysilanes with reactive groups (EtO—Si≡, MeO—Si≡) onto the natural or synthesized clay surface [16–18]. However, in contrast to the alkoxysilanes modified clay, reports on silane-grafted polymer/clay nanocomposite are much less. In this study, we prepare methacryloylpropyltrimethoxysilane (VMMS)-grafted PE (PE-g-VMMS) by melt grafting reaction, and then blend it with organically modified montmorillonite (OMT) to make PE-g-VMMS/OMT nanocomposite. The structure and the thermal-oxidative properties of the nanocomposite are studied by X-ray diffraction (XRD), transmission electron microscopy (TEM), thermogravimetric analysis (TGA) and dynamic Fourier transform infrared spectra (FTIR).

2. Experimental section

2.1. Materials

Low density polyethylene (2102TN26) was obtained from Qilu Petrochemical Company, China. The initiators dicumyl peroxide (DCP) was purchased from Shanghai Experiment Reagent Co. The methacryloylpropyltrimethoxysilane (VMMS) was supplied by Najing Shuguang Chemistry Co. The pristine montmorillonite (MMT) and organophilic montmorillonite (OMT) prepared from MMT by ion exchange reaction using hexadecyl trimethyammounium bromide (C16) were kindly provided by Keyan Chemistry Co.

*Author to whom all correspondence should be addressed.

2.2. Preparation

PE-g-VMMS were prepared by twin-screw extruder with 0.1 phr (part of reagent per hundred parts of LDPE) DCP, and 1.5 phr VMMS. The extruder was operated at 160–200°C. The obtained PE-g-VMMS was pelletized and dried at 80°C. The dried pellets were then premixed with 5 wt% MMT (dried) or OMT (dried), the two composites were then blended by two-roll mill at 160°C for 10 min.

2.3. Characterization

X-ray diffraction (XRD) patterns were performed on the 1mm thick compression moulded films with a Japen Rigaku D/Max-Ra rotating anode X-ray diffractometer equipped with a Cu K_α tube and Ni filter ($\lambda = 0.1542$ nm). Transmission electron microscopy (TEM) images were obtained on a Jeol JEM-100SX transmission electron microscope with the acceleration voltage of 100 kV. The nanocomposite specimen was cut at room temperature using an ultramicrotome (Ultracut-1, UK) with a diamond knife from an epoxy block with the films of the nanocomposite embedded.

Thermogravimetric analyses (TGA) were conducted with a Netzsch STA 409C thermoanalyzer instrument. In each case, the 10 mg specimens were heated from 25 to 700°C using a linear heating rate of 10°C/min under air flow.

The Fourier transfer infrared (FTIR) spectra were scanned using a Nicolet MAGNA-IR 750 spectrometer for characterization of silane-grafted PE. The dynamic FTIR spectra were recorded by the spectrometer equipped with a heating device. The film samples were placed in a ventilated oven at a heating rate of 10°C/min for the dynamic measurement of FTIR spectra in the condensed phase during the thermo-oxidative degradation.

3. Results and discussion

3.1. FTIR characterization

Fig. 1 displays the FTIR spectra of pure PE and VMMS-grafted PE. The resulting grafted PE shows two new absorption bands at 1092 and 1724 cm^{-1}, which are the characteristic wavenumbers of the group Si─O─CH_3 and the carbonyl groups, respectively [14]. The results confirm the grafting of VMMS onto PE.

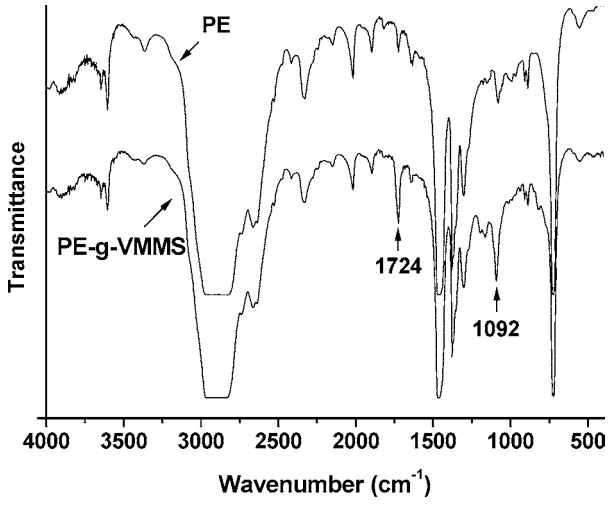

Figure 1 FTIR spectrum of PE and PE-g-VMMS.

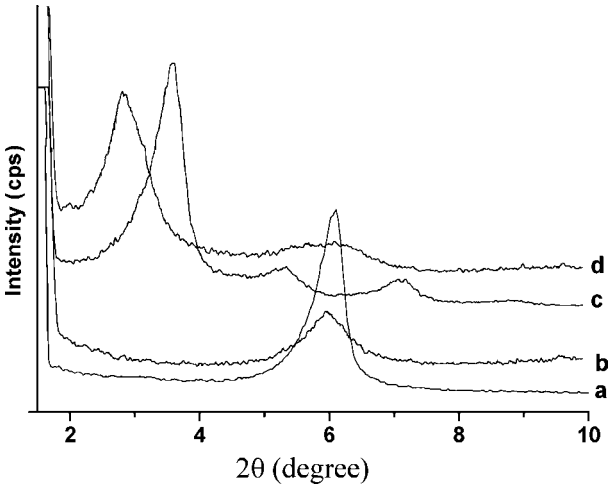

Figure 2 XRD patterns for (a) MMT, (b) PE-g-VMMS/MMT, (c) OMT, and (d) PE-g-VMMS/OMT.

3.2. Morphological structure

Fig. 2 shows XRD profiles of MMT, OMT, and PE-g-VMMS based composites containing 5 wt% of MMT and OMT. Fig. 2a represents a typical XRD pattern of pristine MMT with the (001) plane reflection peak at about 6°, corresponding to the basal spacing 1.5 nm, while the diffraction peak of PE-g-VMMS/MMT sample (Fig. 2b) does not shift to lower angle, indicating the system is still a conventional composite. The average basal spacing of OMT (Fig. 2c) increased from 1.5 nm to 2.5 nm compared with MMT, suggesting the chain of C16 intercalates into the MMT galleries and expands them. The PE-g-VMMS/OMT hybrid (Fig. 2d), it exhibited a broadened spacing at 3.2 nm, the 0.7 nm gallery height increase indicates intercalation of PE-g-VMMS into the silicate interlayer had taken place and a nanocomposite structure was obtained.

Fig. 3 shows the TEM micrograph of the PE-g-VMMS/5 wt% OMT nanocomposite. It clearly demonstrates that it has a typical intercalated silicate tactoids nanomorphology with little disorder in the layers. The intercalated structures are characterized by

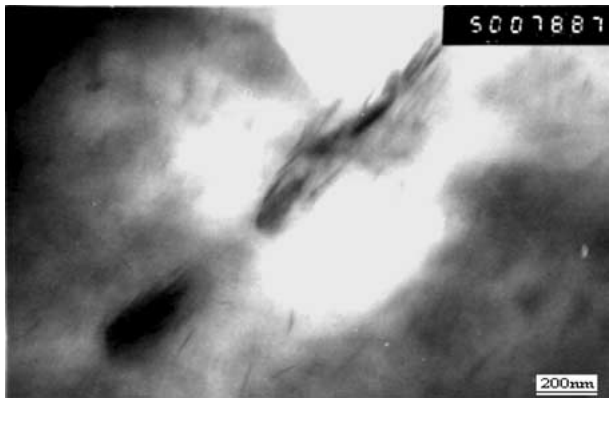

Figure 3 TEM image of PE-g-VMMS/5 wt% OMT nanocomposite.

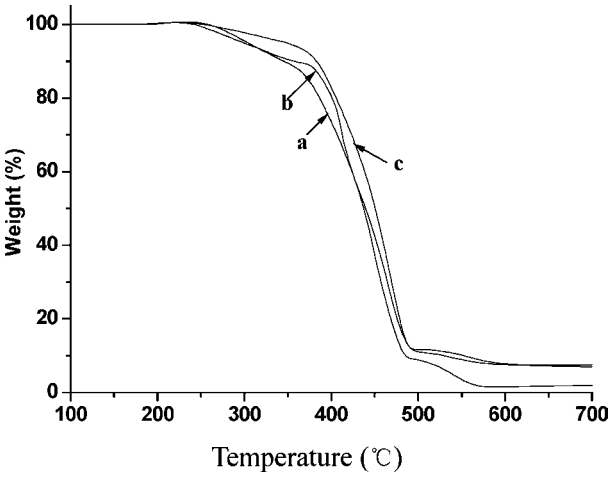

Figure 4 TG curves for (a) PE-g-VMMS, (b) PE-g-VMMS/5 wt% MMT, and (c) PE-g-VMMS/5 wt% OMT under air flow.

a parallel registry that gives rise to the XRD reflection of Fig. 2, whereas the disordered state of silicate layers have no periodic stacking and thus remain XRD silent [19], which results in decreased intensity in the peak of LDPE-g-VMMS/OMT nanocomposite compared with OMT.

3.3. Thermal-oxidative characteristics

Fig. 4 illustrates the TGA curves of pure PE-g-VMMS, PE-g-VMMS/5 wt% MMT microcomposite and PE-g-VMMS/5 wt% OMT intercalated nanocomposite. The detailed data corresponding to the temperature point at which 5% ($T_{5\%}$) and 50% ($T_{50\%}$) thermal-oxidative degradation occurs are tabulated in Table I.

During the thermal-oxidation degradation, TG curves for all samples show a slight weight increase in the temperature range from 150 to 250°C, this phenomenon can be explained by the fact that silane crosslinking occurs in the presence of oxygen [15]. $T_{5\%}$ occurs at 304°C for pure PE-g-VMMS. PE-g-VMMS/MMT microcomposite does not show any increase in $T_{5\%}$, whereas PE-g-VMMS/OMT nanocomposite exhibits apparent 42°C enhancement in the thermal-oxidative stabilization effect. In comparison with the weight loss in the temperature range from 250 to 375°C, 16% weight loss of PE-g-VMMS occurs due to the volatilization of thermo-oxidative degradation products, while about 11% and only 8% weight loss is observed in microcomposite and nanocomposite, respectively. On elevating the temperature from 375 to 500°C, the weight loss rate of both PE-g-VMMS and its composites increased rapidly, and the nanocomposite showed higher thermal-oxidative stability. When comparing $T_{50\%}$, the temperatures are 435, 439 and 447°C for PE-g-VMMS, microcomposite and nanocomposite, respectively. The results indicate that for the sample investigated here in, PE-g-VMMS/OMT nanocomposite shows higher thermal stability than pure PE-g-VMMS and the microcomposite, but it exhibits less improvement in the thermal-oxidative stability effect above 375°C than that in the temperature range from 250 to 375°C.

TABLE I Thermal properties of PE-g-VMMS, PE-g-VMMS/MMT microcomposite and PE-g-VMMS/OMT nanocomposite under air flow

Sample	$T_{5\%}$ (°C)	$T_{50\%}$ (°C)
PE-g-VMMS	304	435
PE-g-VMMS/5 wt% MMT	304	439
PE-g-VMMS/5 wt% OMT	346	447

The variation of the thermal-oxidative stabilization effect imparted by silicates to PE-g-VMMS is likely to be attributed to physico-chemical effect between the polymer and the silicate layers. It is found that 1–2 wt% water is contained in the OMT although it is considered hydrophobic [20], the siloxane groups (—$Si(OCH_3)$) attached on polymer chains hydrolyze with the water to silanol groups (—Si(OH)), then interact with the hydroxyl groups presented at the layer edge forming hydrogen bonds [16]. On elevating the temperature, the hydrogen bonds convert to siloxane bonds with silicate surface through condensation [17], consequently, PE-g-VMMS are covalently bonded with the surface of silicate layers. Therefore, the layers with high aspect ratio are able to hinder the mobility of the macromolecular chains and work as a shield to retard the heat diffusion into the substrate and delay the volatilization of the thermal-oxidative product. The improvement of the thermal-oxidative stability of nanocomposite comparatively to the microcomposite is due to the molecular dispersion of silicate layers in the PE-g-VMMS increasing the amount of covalently bonds and thus enhancing the interfacial action between the polymeric matrix and silicate layers.

Thermal decomposition of alkyl quaternary ammonium montmorillonite takes place between 200–400°C with Hofmann mechanism forming Lewis acid sites in the aluminosilicate, which have a catalytic effect on the degradation of organics within the OMT [20]. The insignificant improvement in thermal-oxidation degradation of the nanocomposite at high temperature might be explained by the catalytic effect of the sites in the degradation process of PE-g-VMMS, especially in the existence of the acyloxy group of the pendant VMMS grafts, which is expected to have a deleterious effect on thermal stability.

3.4. Dynamic FTIR characteristic

Dynamic FTIR spectra are used to investigate the details of the thermo-oxidative behavior of the samples. Fig. 5 presents the dynamic FTIR spectra obtained from the pure PE-g-VMMS (Fig. 5A) and PE-g-VMMS/5 wt% OMT nanocomposite (Fig. 5B) at different pyrolysis temperatures. The two important bands we are concerned are located in the region of 2800–3000 cm^{-1} and about 1720 cm^{-1}. The first bands in the 2800–3000 cm^{-1} range are the characteristic frequency of the —$(CH_2)_n$ —asymmetric (2927 cm^{-1}) and symmetric (2855 cm^{-1}) vibration, decrease with the increasing temperature. However, the relative peak intensities of PE-g-VMMS/OMT nanocomposite are much higher than pure LDPE-g-VMMS at the same temperature,

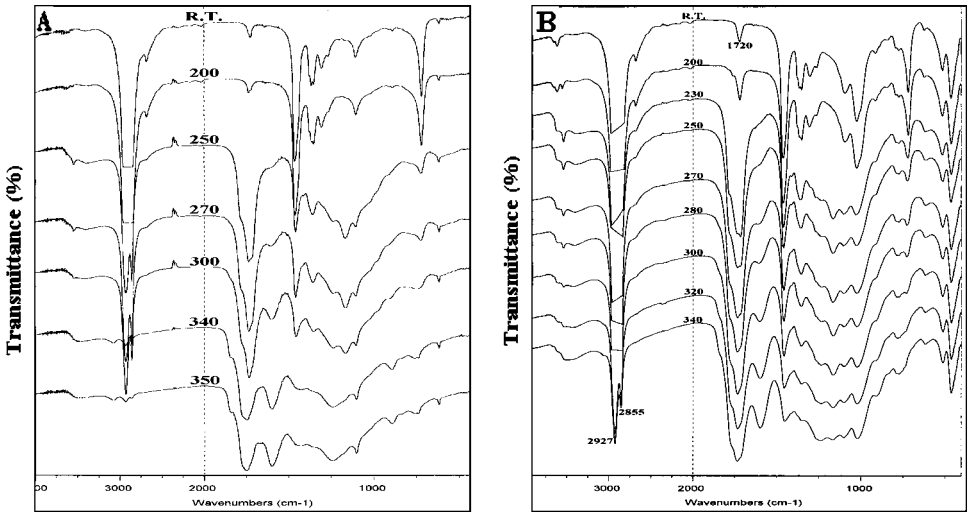

Figure 5 Dynamic FTIR spectra at different pyrolysis temperatures: (A) LDPE-g-VMMS and (B) LDPE-g-VMMS/5 wt%OMT nanocomposite.

reveals the nanocomposite has a slower thermo-oxidative rate of the main chains than that of pure PE-g-VMMS.

The second band lies at about 1720 cm^{-1}, assigned to the various C=O thermo-oxidative products, increasing sharply as pyrolysis temperature elevates. However, the nanocomposite shows higher relative peak intensities than those of pure PE-g-VMMS at the corresponding pyrolysis temperatures, indicating a faster thermo-oxidative rate of C=O production. Considering that the silicate layers slow down the thermo-oxidative rate of PE-g-VMMS main chains, the faster generation of C=O products is attributed to the Lewis acid sites promoting the thermal-oxidative rate of the pendant VMMS grafts.

4. Conclusion

The intercalated PE-g-VMMS nanocomposite was prepared by melt blending PE-g-VMMS and OMT. The studies of thermal characteristics revealed that the PE-g-VMMS/OMT nanocomposite showed high thermal-oxidative stability at 250–375°C, but the composites did not show significant improvement at higher temperature. It is noteworthy that the physico-chemical effect between the PE-g-VMMS and the OMT has an important role in the thermal-oxidative degradation process. The silicate layers covalently bonded onto the macromolecular chains improve the thermal-oxidative stability of nanocomposite while the Lewis acid sites enhance the thermal-oxidative degradation rate of the pendant VMMS grafts. The influence of silicate layers on the characteristics of the resulting silane-grafted water-crosslinked polyethylene needs further investigation.

Acknowledgement

The work was financially supported by the China NKBRSF project (No. 2001CB409600).

Received 12 April
and accepted 1 July 2004

References

1. M. ALEXANDRE and P. DUBOIS, *Mater. Sci. Eng.* **28** (2000) 1.
2. A. OKADA, M. KAWASUMIC, A. USUKI, Y. KOJIMA, T. KURAUCHI and O. KAMIGAITO, *Mater. Res. Soc. Proc.* **171** (1990) 45.
3. K. DIRK, T. RALF and M. ROLF, *Polymer.* **43** (2002) 2909.
4. H. L. XIAO and J. W. QIU, *ibid.* **42** (2001) 10013.
5. A. MICHAEL, D. PBILIPPE, S. TAO, M. G. JUAN and J. ROBETT, *ibid.* **43** (2002) 2123.
6. T. G. GROPAKUMAR, J. A. LEE, M. KONTOPONLON and J. S. PARENT, *ibid.* **43** (2002) 5483.
7. X. L. JIAN, S. W. JING and M. C. CHI, *ibid.* **41** (2000) 6935.
8. T. LAN, P. D. KAVIRATNA and T. J. PINNAVAIA, *Chem. Mater.* **7** (1995) 2144.
9. M. KATO, A. USUKI and A. OKADA, *J. Appl. Polym. Sci.* **66** (1997) 1781.
10. M. KAWASUMI, N. HASEGAWA, M. KATO, A. USUKI and A. OKADA, *Macromolecules.* **30** (1997) 6333.
11. Y. KUROKAWA, H. Y. ASUDA and A. OYA, *J. Mater. Sci. Lett.* **16** (1997) 1670.
12. N. HASEGAWA, M. KAWASUMI, M. KATO, A. USUKI and A. OKADA, *J. Appl. Polym. Sci.* **67** (1998) 87.
13. T. S. YEONG and H. T. TE, *ibid.* **69** (1998) 255.
14. H. HUANG, H. H. LU and N. C. LIU, *ibid.* **78** (2000) 1233.
15. A. M. JULIE, R. R. JOSEPH, C. R. HWANG and A. K. SAAD, *J Polym. Sci: Part B.* **38** (2000) 2468.
16. X. KORNMANN, in "Synthesis and Characterisation of Thermoset-Clay Nanocomposites" (Lulea University of Technology, Sweden, 1999) p. 10.
17. C. M. LEU, Z. W. WU and K. H. WEI, *Chem. Mater.* **14** (2002) 3016.
18. K. A. CARRADO, L. Q. XU, R. CSENCSITS and J. V. MUNTEAN, *ibid.* **13** (2001) 3766.
19. E. MANIAS, A. TOUNY, L. WU, K. STRAWHECKER, B. LU and T. C. CHUNG, *ibid.* **13** (2001) 3516.
20. W. XIE, Z. M. GAO, W. P. PAN, D. HUNTER, A. SINGH and R. VAIA, *ibid.* **13** (2001) 2979.